Festkörperprobleme 29 (1989)

Pattern Formation in a Liquid Crystal

Ingo Rehberg, Bernhard L. Winkler, Manuel de la Torre Juarez, Steffen Rasenat, and Wolfgang Schöpf

Physikalisches Institut, PF 101251, Universität Bayreuth, D-8580 Bayreuth, FRG

Summary: Applying a voltage to a nematic liquid crystal sandwiched between two electrodes leads to convection when a critical threshold value of the driving voltage is exceeded. The patterns arising above this threshold are studied experimentally. Special emphasis is put on an instability leading to travelling waves and the role of defects on the route to turbulence.

1 Introduction

The problem of pattern formation in nonequilibrium systems obviously is the most important one in science: The formation of life on earth can simply be understood by assuming an ensemble of chemical compounds driven out of equilibrium by the radiation of the sun [1]. In order to understand some features of pattern formation processes, which are observed in many different fields including biology, chemistry and physics [2], one needs to deal with simpler systems. Within physics the motivation to study order-disorder transitions certainly has led to a renaissance of classical fluid dynamics during the last decade. The hydrodynamic instabilities offer the experimental advantage to allow reproducible measurements with well defined boundary conditions. For the theoretical physicist they offer the advantage to be based on well-defined theoretical grounds, the Navier-Stokes equations. The most popular hydrodynamic instabilities are circular Couette flow going unstable with respect to Taylor vortices [3] and Rayleigh-Bénard

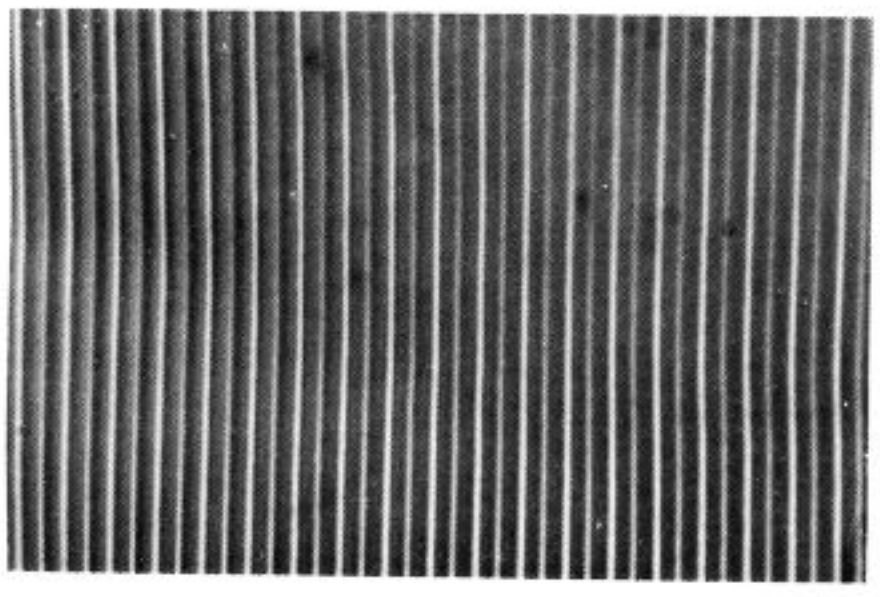

Fig. 1 Image of Williams rolls (7 V)

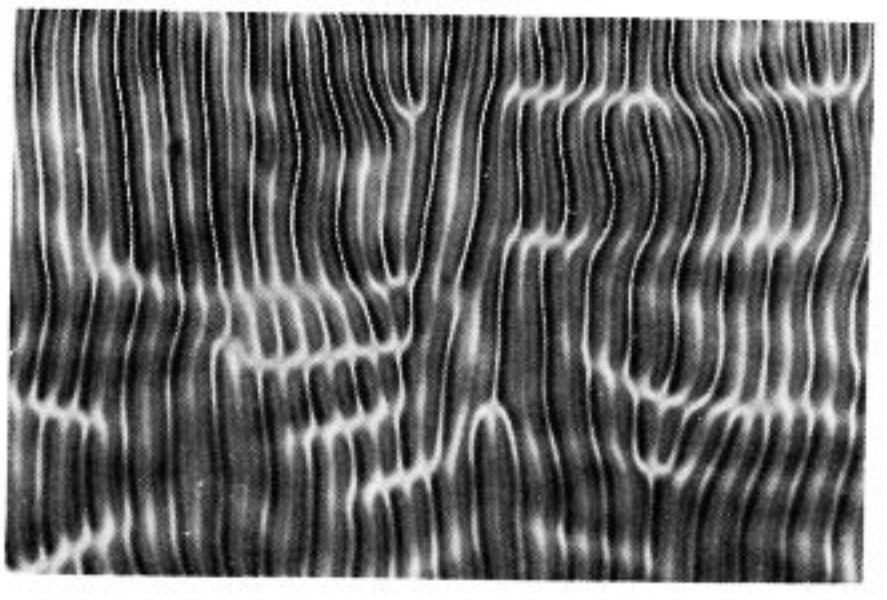

Fig. 2 Fluctuating Williams rolls (10 V)

convection [4]. A special case of the latter is thermal convection in a binary mixture, where the thermal expansion competes with thermodiffusion leading to an oscillatory instability [5]. In this talk we would like to propose a fluid dynamical system as useful for studies in pattern formation which can not exactly be called classical: Convection patterns in an anisotropic fluid, namely a nematic liquid crystal (Figs. 1 and 2). In the experiments presented here the convection is driven by an electric field, thus it is called electro-hydrodynamic convection (EHC) [6].

Many pattern forming instabilities including the ones mentioned above share a common scenario summarized in Fig. 3. The system is driven from equilibrium by means of a control parameter, for example a chemical concentration, a Reynolds number, a temperature difference or a voltage. The transition from the ground state to the structured state takes place at a well defined value of the control parameter. Above this threshold the order parameter of the system, which might be a velocity, a temperature or a director angle in the case of EHC, is different from zero. We concentrate here on systems where this upper state shows up as a periodic pattern. Above the transition point a wavenumber band exists as indicated by the upper part of Fig. 3. Theoretical descriptions of pattern forming instabilities generally start with a linear stability analysis of the spatially homogenous ground state. The amplitude of the most unstable mode might then be described by means of a weakly nonlinear analysis leading to an amplitude equation. The results

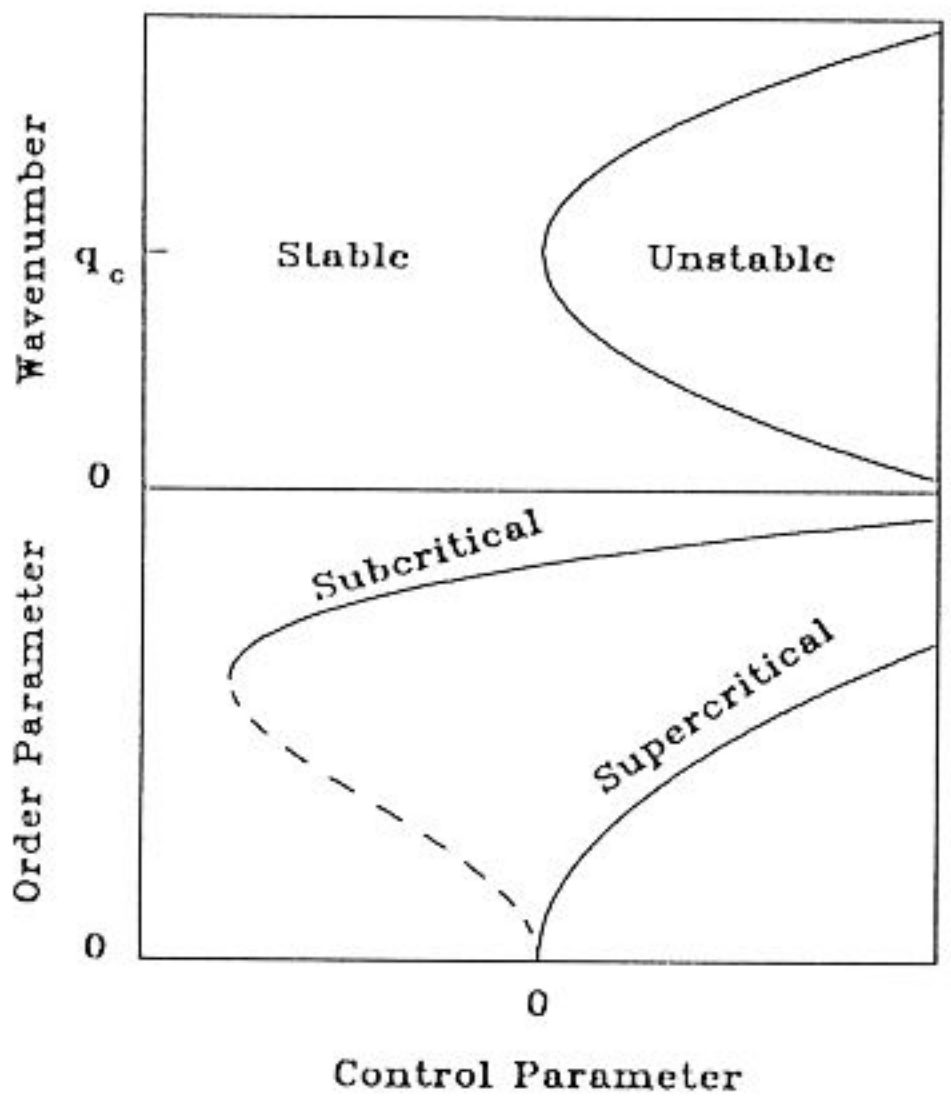

Fig. 3 Bifurcation scenario of pattern forming instabilities. At a well-defined value of the control parameter the system looses stability to a periodic structure with the wavenumber q_c. The bifurcation is called subcritical if the bifurcating branch extends to negative values of the control parameter, otherwise supercritical.

of the application of this concept to electro-hydrodynamic convection are given in [6].

In this paper we deal with experimental aspects of EHC. In section 2 the experimental methods used to explore EHC are described. The possible patterns arising above the convection threshold are then displayed in section 3. Increasing the voltage leads to a higher degree of disorder, which might manifest itself in more complicated, but regular patterns, or in an increasing number of defects as shown in Fig. 2. In section 4 we concentrate on more recent and special results: The observation of travelling waves, which are unexpected on the basis of the accepted theory for EHC, and the defect statistics in the weakly turbulent regime.

2 Experimental Set-up and Procedure

The experimental set-up is shown in Fig. 4: the nematic liquid crystal is sandwiched between two transparent, indiumoxid coated glass eletrodes. As the working fluid, we use either the nematic N-(p-methoxybenzylidene)-p-butylaniline (MBBA) or the Merck Phase V, a mixture of azoxy compounds. The former offers the advantage that the material parameters have been measured extensively. Phase V on the other hand is more convenient to observe oblique rolls, a different convection pattern which will be described in more detail in chapter 3. The spacing between the two electrodes ranges from 10 to 100 micrometer. The nematic is in the so called planar orientation: the director of the fluid is parallel to the plates. A preferred orientation (along the y axis) is achieved by rubbing the electrodes. Because all the material parameters of the liquid crystals are temperature dependent, it is neccesary to stabilize the temperature of the cell. We reach a stability of ± 0.005 K by means of a water circuit. The cell is mounted on a polarizing microscope for flow visualisation.

Applying an ac-voltage across of the cell leads to convection when a certain value of that voltage is exceeded. The convection shows up in the form of parallel rolls as indicated in Fig. 4. Adjacent rolls have different sense of rotation. The deformation of the director field is also indicated in Fig. 4. If

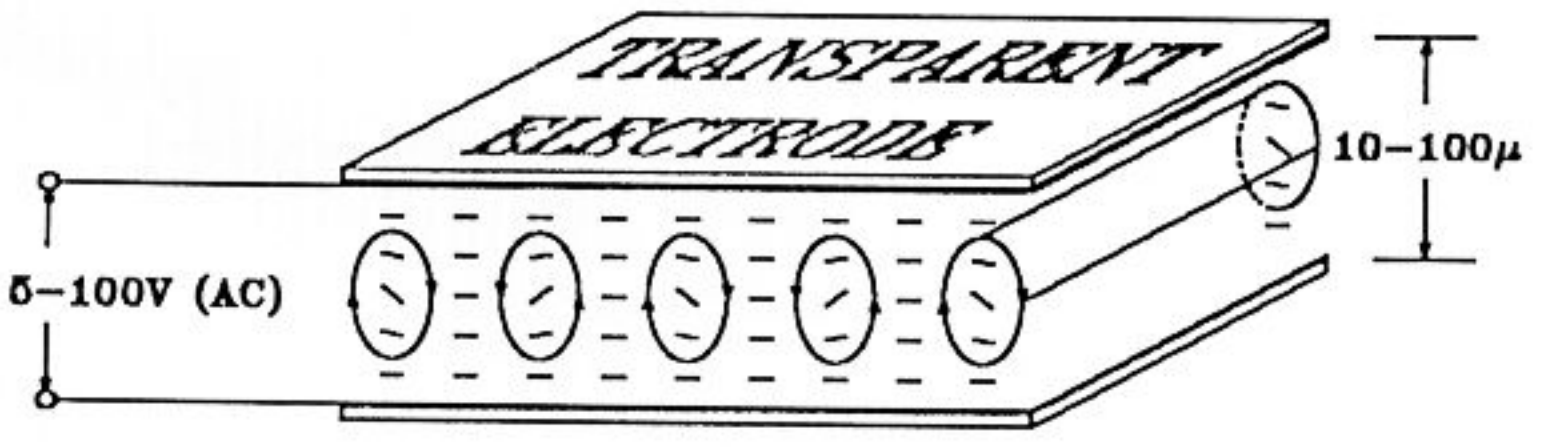

Fig. 4 The convection cell. The transparent electrodes have a typical spacing between 10–100 μm. The director orientation is indicated by (–); the streamlines by the circles.

light polarized parallel to the director is sent through the cell, an image of the convection pattern is formed as shown by the photograph 1. This visualisation method is a special case of the well known shadowgraph method: The light beams are bent inside the cell leading to intensity modulations. In the usual shadowgraph method, density gradients cause the deflection. In EHC, however, one deals with refraction of the extraordinary light inside the liquid crystal. A discussion of the differential equation describing the path of light inside the cell is given in [7]. If the optical anisotropy and the orientation of the optical axis (i.e. the orientation of the director) inside the cell are known, the path of the light and the intensity behind the cell can be calculated. Figure 5 shows the result of such a numerical calculation of the light path inside the cell. The most important result of the calculations presented in [7] is the fact that the angle of the outgoing light grows with the square of the director angle θ, but the light deviation inside the cell and therefore the intensity modulation measured behind the cell contain a term linear in θ. This linear term is responsible for creating different images of the upflow (broad intensity maxima in Fig. 1) and downflow (sharp maxima in Fig. 1). Figure 6 shows a measurement of this modulation as a function of the driving ac-voltage. From the measured intensities and the shape of the intensity curves a number proportional to the angle θ of the director field can be extracted, and the result is shown in Fig. 7. The solid line is a fit to the square root law expected for this supercritical bifurcation due to symmetry arguments.

The optical methods can be used for time dependent studies as well. In Fig. 8 a voltage step from a subcritical value without convection to a supercritical value and steps from a supercritical value to 3 different subcritical values have been applied. The intensity modulation along a line perpendicular to the axis of the rolls is plotted as a function of time. The amplitude grows or decays exponentially for small values. This growth or decay time increases when approaching the critical point. This behaviour is the analogue to the critical slowing down in equilibrium phase transitions.

$$\frac{\partial f}{\partial y} - \frac{\partial^2 f}{\partial y' \partial x} - \frac{\partial^2 f}{\partial y' \partial y} \cdot y' - \frac{\partial f^2}{\partial y'^2} \cdot y'' = 0$$

$$f(x,y,y') = n(x,y,y') \cdot (1+y'^2)^{1/2}$$

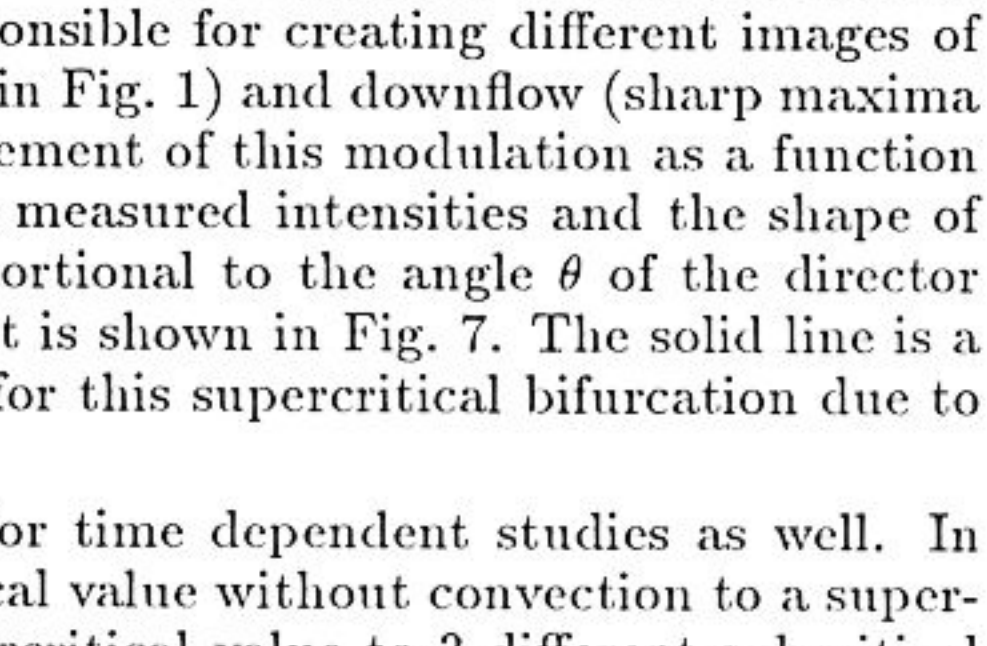

Fig. 5 The light path inside the convecting fluid is calculated using the streamfunctions obtained by linear stability theory and the differential equation describing the path of the extraordinary light.

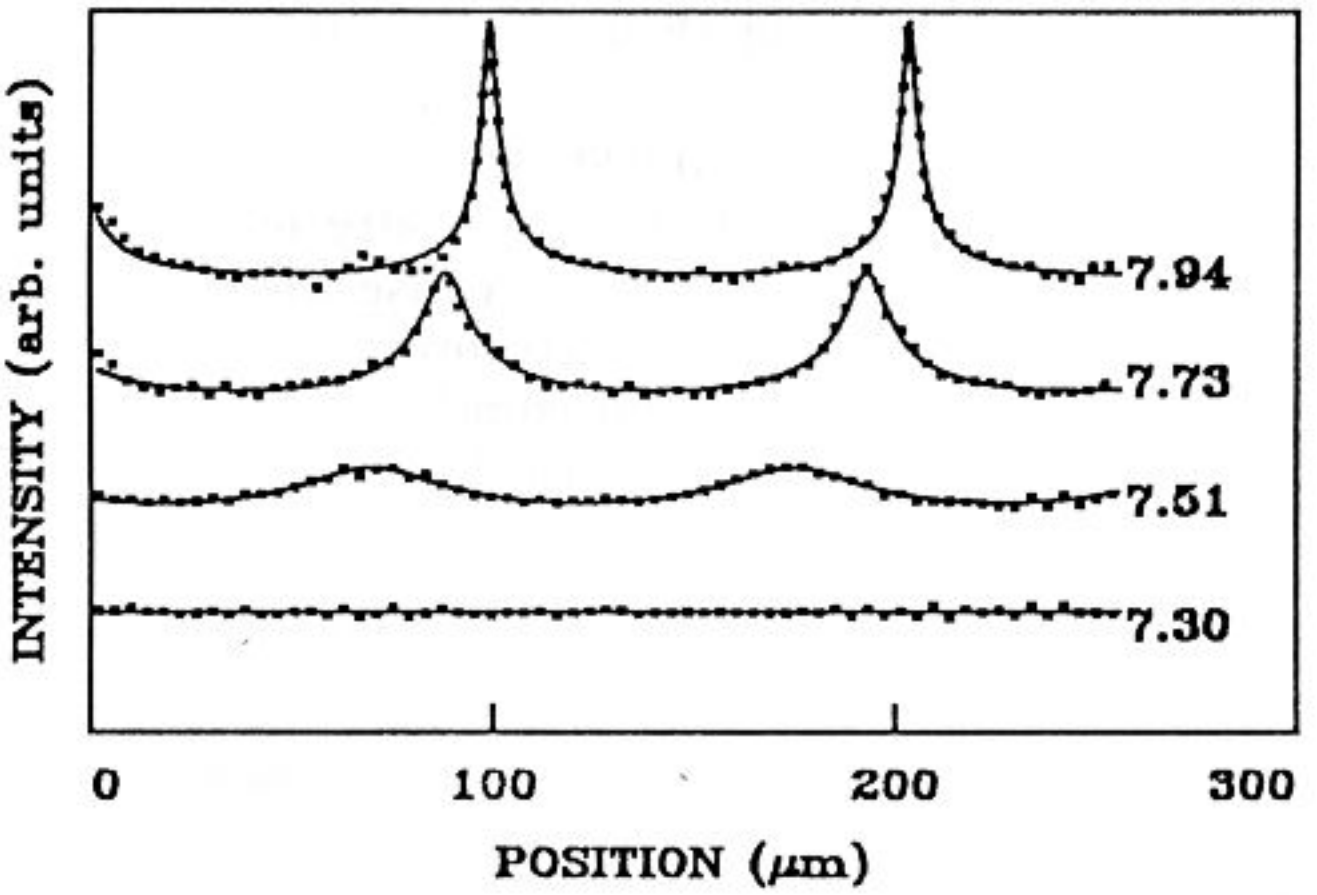

Fig. 6 The intensity measured for different driving voltages in a cell of 100 μm thickness.

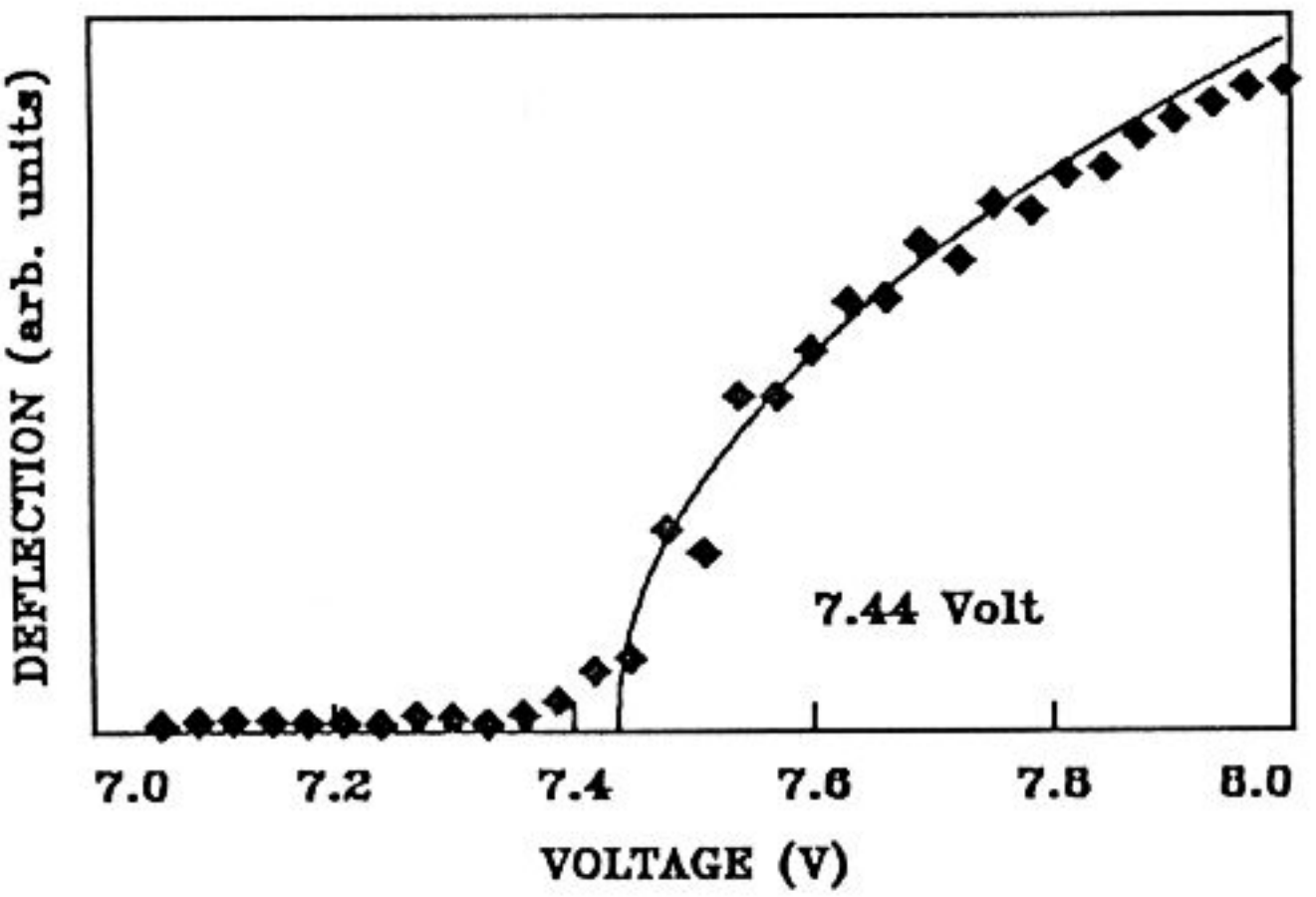

Fig. 7 Order parameter extracted from the intensity measurements shown in Fig. 6. The absolute distance of the focal plane of the microscope from the cell is not known exactly, thus arbitrary units are given for the deflection of the light inside the cell. This value, however, is proportional to the tilt angle θ of the director and thus a suitable order parameter.

As an alternative to the optical methods described above, electrical methods can be used. From this point of view, the cell can be considered as a capacitance parallel to an electric resistance. If not only the voltage, but also the electrical current flowing into the cell and the phase between both is measured for different driving frequencies below the onset of convection,

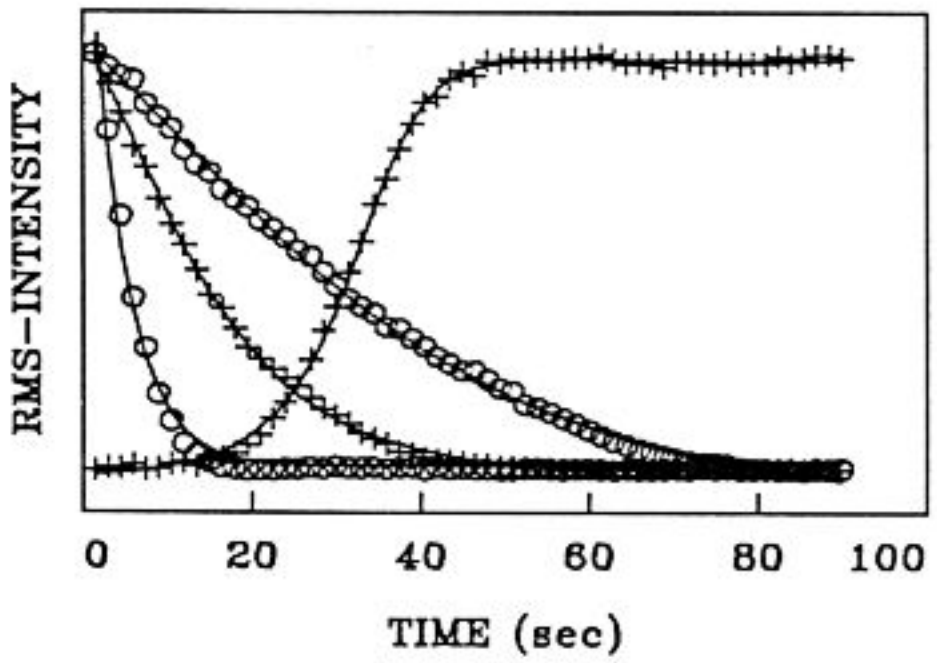

Fig. 8 Time dependence of the order parameter for different voltage steps, namely to 11.78 V (supercritical), 11.06 V, 11.03 V and 10.78 V (subcritical values), 30 Hz.

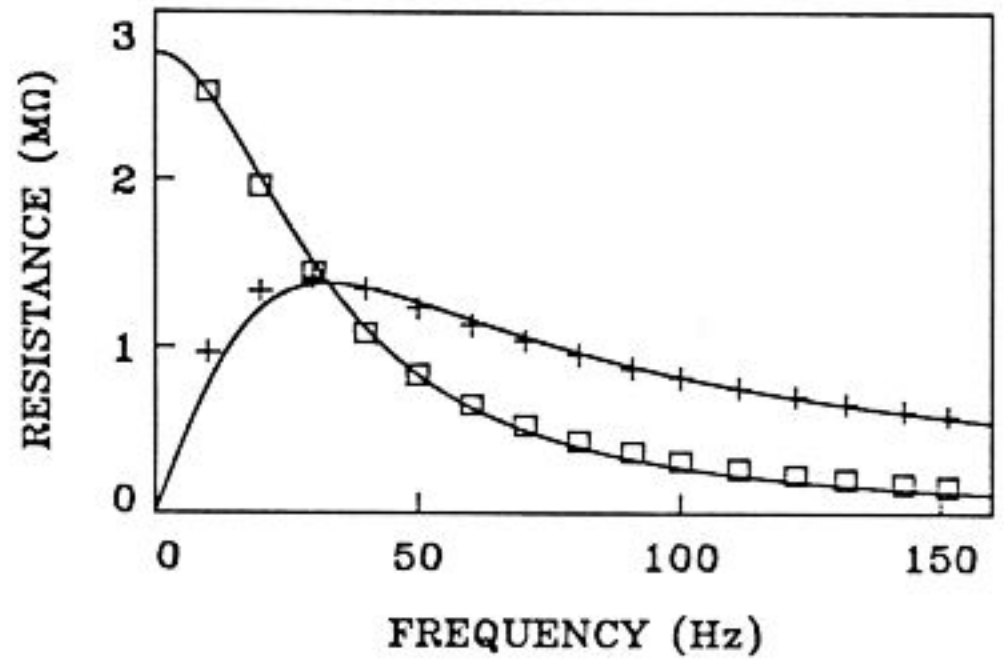

Fig. 9 Real (squares) and imaginary (plus) part of the resistance measured at a subcritical *ac*-voltage of 4.5 V RMS.

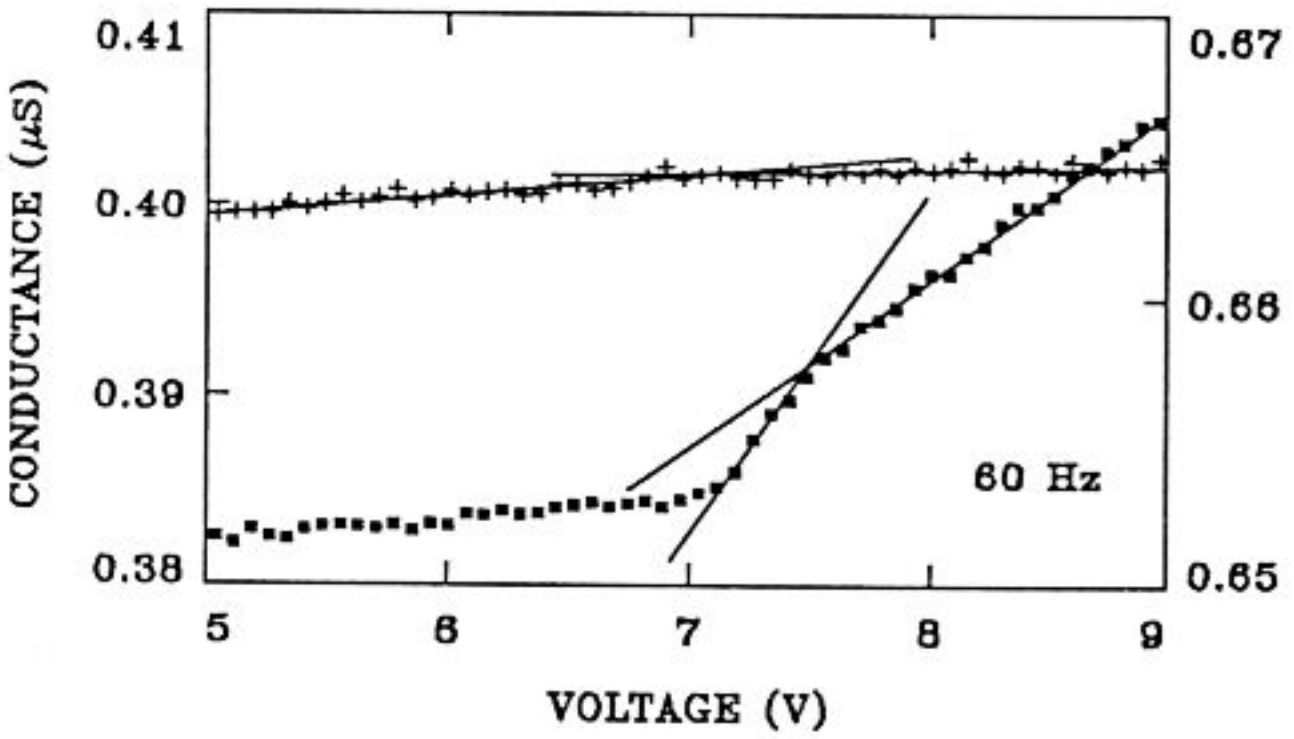

Fig. 10 The real (squares, left hand side labels) and imaginary (crosses) conductance measured as a function of the driving voltage at 60 Hz. The change of the slope indicates the onset of convection or a secondary instability.

both the resistive part and the capacitance can be extracted as demonstrated in Fig. 9. The onset of convection can be detected as an increase in the electrical conductance of the cell. This measurement is the analogue of the heat transport measurements in thermal convection. Figure 10 shows an example. Both the resisistive part (current and voltage in phase) and the imaginary part (phase difference 90 degrees) have been plotted as a function of the driving voltage. The increase in the resistive part reflects the fact that power is needed to drive the convection of the fluid. The change of the imaginary part does not have such a simple physical interpretation. It can be positive or negative depending on the driving frequency.

3 Pattern Formation

The convection pattern shown in Fig. 1 is not the only one possible in EHC. In fact, the kind of pattern appearing at threshold depends on the nematic used, its temperature, its electrical conductivity, the thickness of the cell and the frequency of the driving voltage. Figure 11 shows the

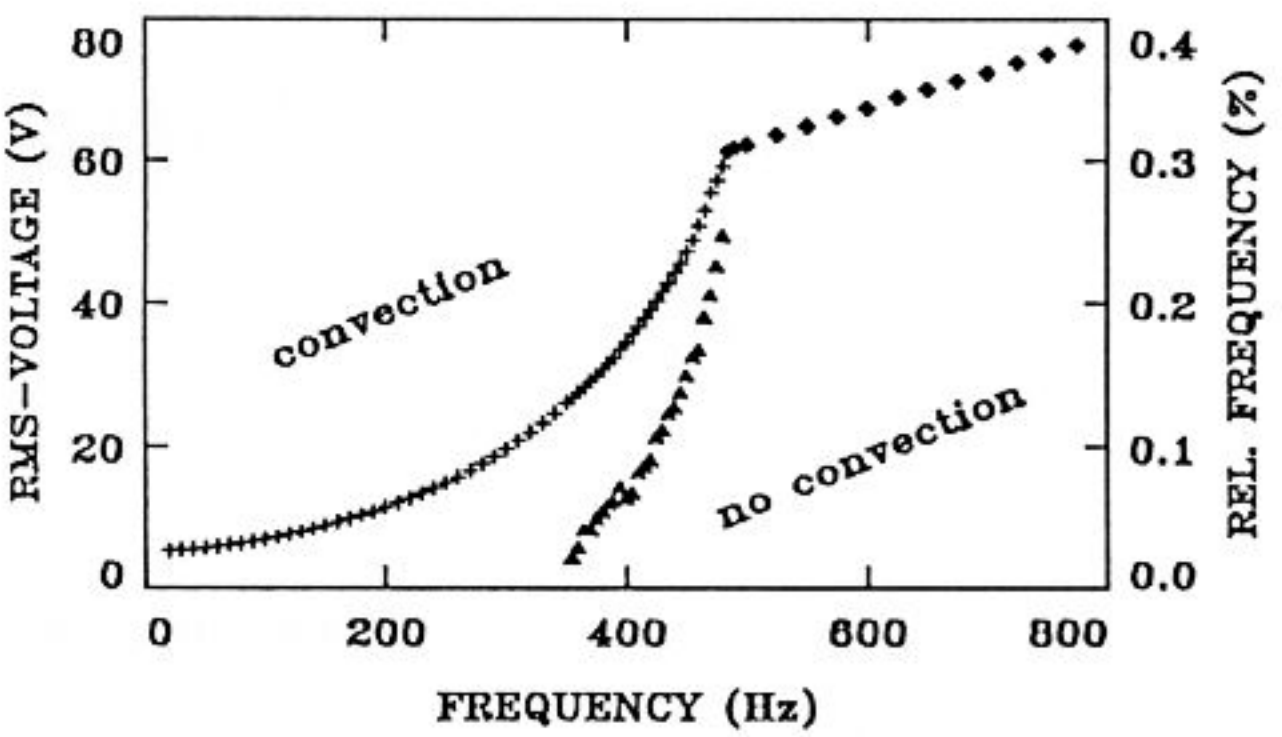

Fig. 11 Phase diagram for a 15 μm Phase V cell. Below 350 Hz convection sets in as a steady pattern, between 350 Hz and 420 Hz it starts as a moving pattern with the frequency given by the triangles; above 420 Hz dielectric rolls appear.

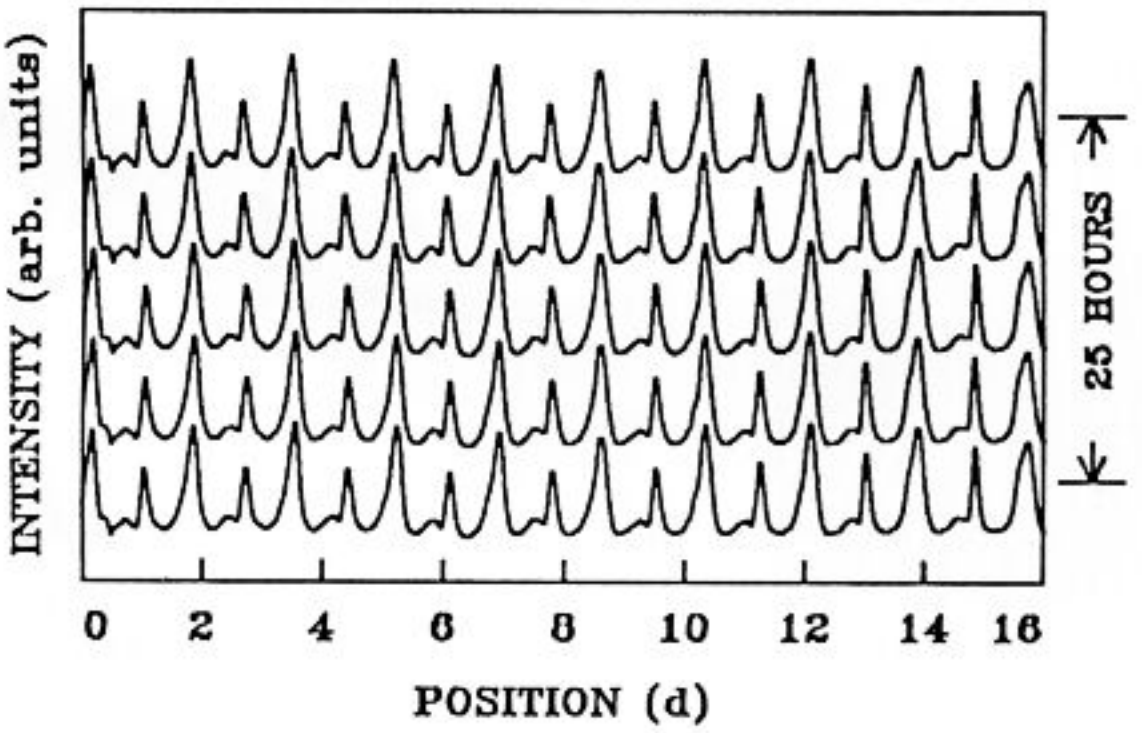

Fig. 12

Time-dependence of steady convection rolls.

threshold measurement of a Phase V cell of 15 μm thickness. Here both the threshold voltage and the kind of pattern appearing above threshold are a function of the driving frequency. The simplest pattern occurs at medium frequencies: The stationary Williams rolls shown in Fig. 1. Figure 12 shows a measurement of their time dependence which is a boring one: There is no hint for a movement within 25 hours.

Decreasing the frequency leads to another type of stationary roll pattern: the zig-zags shown in Fig. 13. Here the rolls are not normal to the director like in Fig. 1. They form a finite angle with respect to the normal axis, which becomes smaller when approching a critical frequency, the so called Lifschitz-point [8,9]. For frequencies higher than this critical frequency the rolls are normal to the orientation of the director.

Figure 14 shows a measurement of the angle of the rolls with respect to the axis normal to the director. On the basis of symmetry arguments, one would expect the angle to approach zero at the Lifschitz-point via a square root law. The measurement does not exactly support this statement. On the other hand it is not really contradictory, because all statements stemming from amplitude equations are local ones. The range of applicability of the square root law might be very small in this case.

Increasing the frequency above the normal roll regime leads to another type of instability: Travelling waves occur. They come in like a supercritical bifurcation as demonstrated in the Figs. 15,16. This travelling pattern is not explained by the stability analysis presented in [6]. We will discuss possible explanations in more detail in chapter 4.

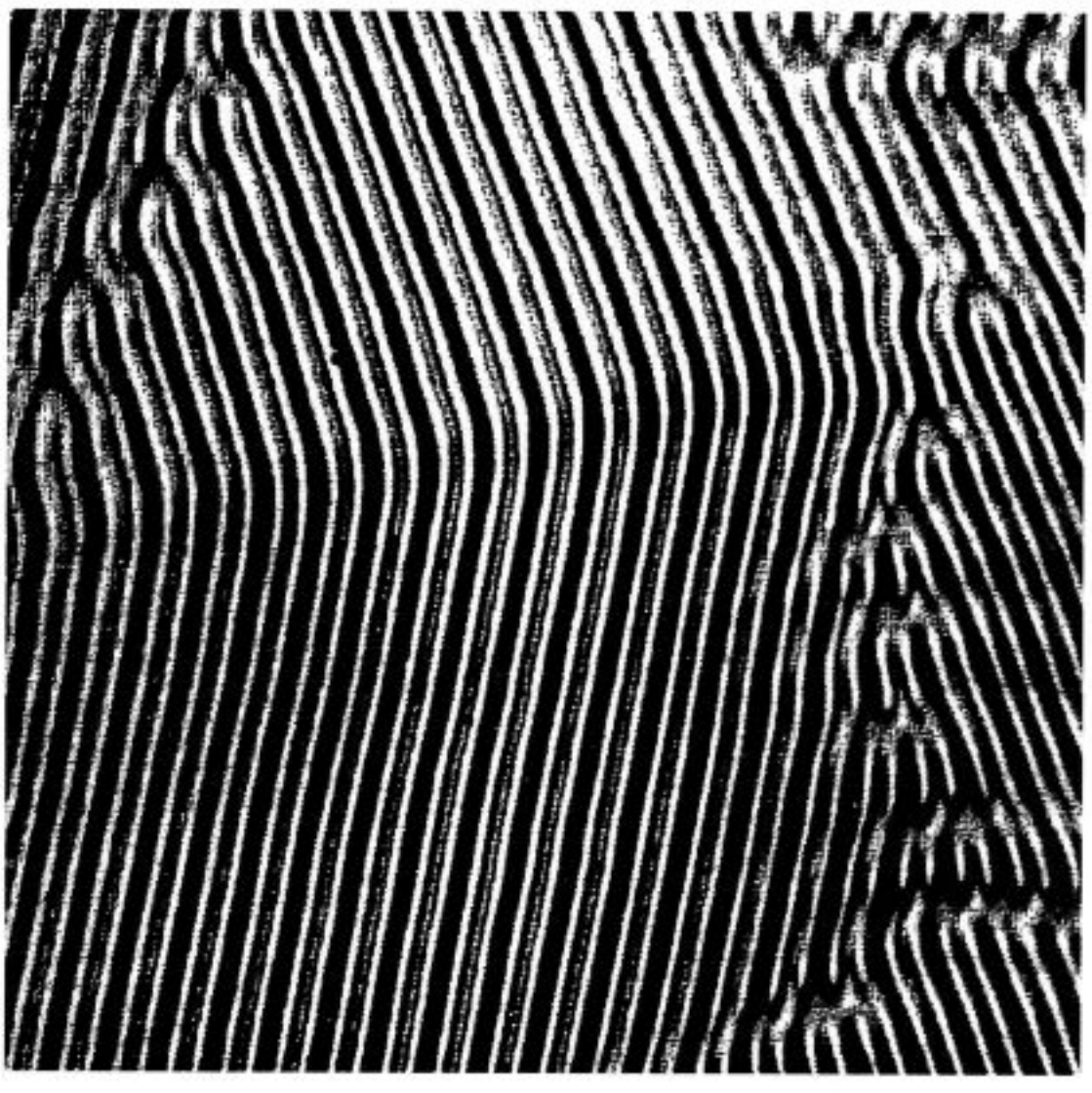

Fig. 13 Image of convection in the oblique roll regime.

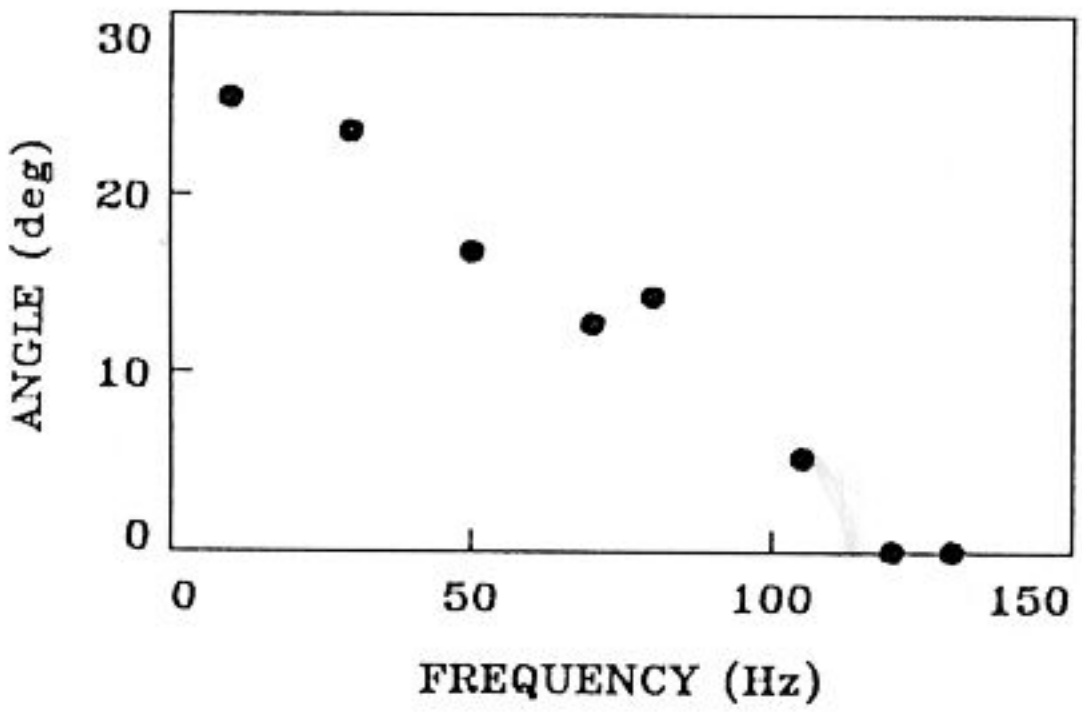

Fig. 14 The angle between "zig and zag" at the onset of oblique rolls.

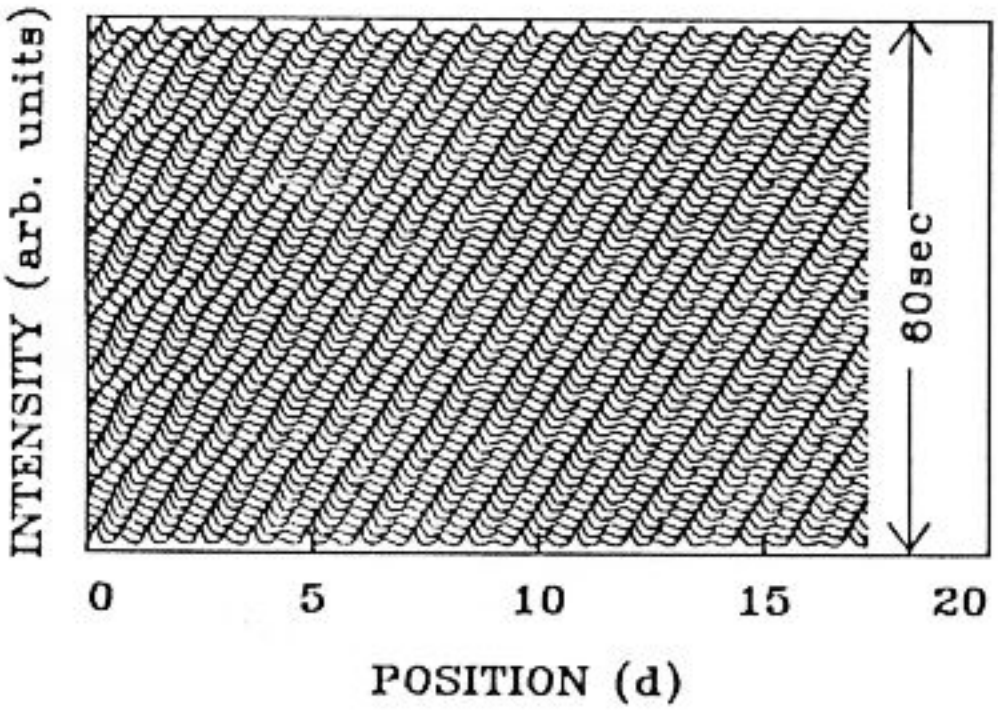

Fig. 15 Travelling waves. Intensity lines measured perpendicular to the roll axis are measured every second and plotted on top of each other.

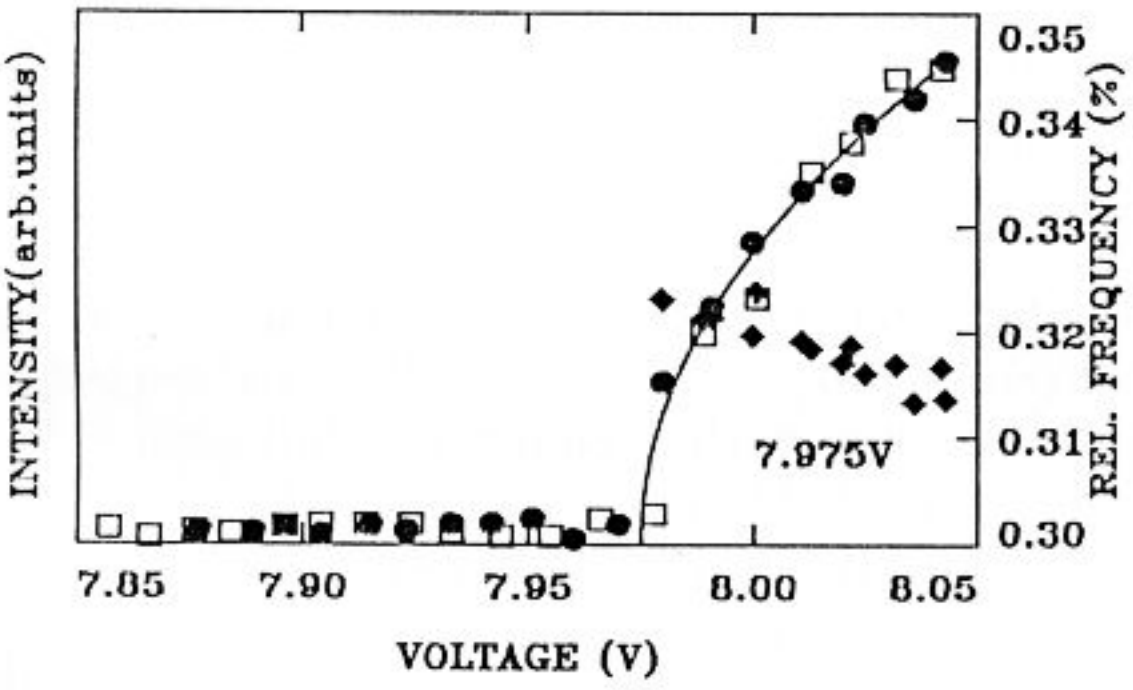

Fig. 16 Amplitude (squares: increasing voltage, circles: decreasing voltage) and frequency (diamonds) of TW. The amplitude grows continuously following a square root law; and the frequency comes in at a finite value.

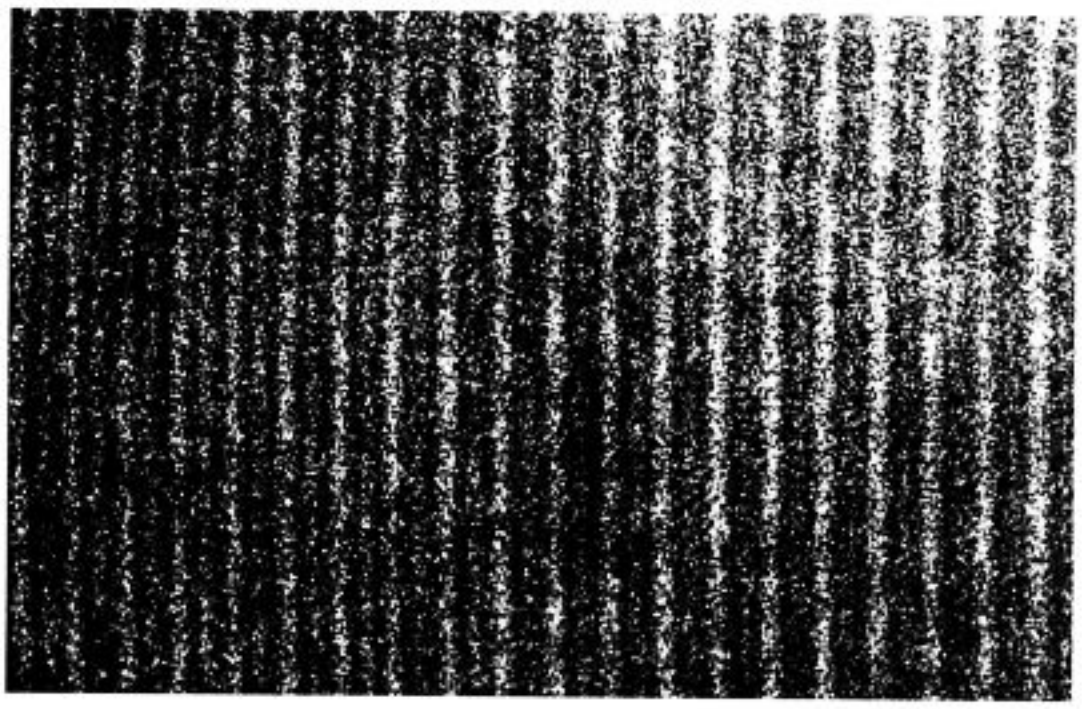

Fig. 17 Image of dielectric rolls obtained with stroboscopic illumination.

At higher frequencies the first instability to occur are the so called dielectric rolls. The difference between the low-frequency and the high frequency regime is illustrated nicely in [10]: In the first state, the director and flow fields are approximately stationary within one period of the external driving, while in the dielectric regime these fields oscillate following the external frequency. This fact makes dielectric rolls hard to observe, because the linear light modulation is averaged to zero in time. This difficulty can be overcome with stroboscopic illumination, which had been used to take the photograph 17.

The patterns shown up to now bifurcate directly from the homogenous ground state, i.e. it should be possible to describe them by means of a linear stability theory. If the driving voltage is increased beyond the critical one, one would expect the amplitude of the director field and the velocity to grow according to a square root law as already indicated in Fig. 7. Predicting the magnitude of this growth requires a nonlinear amplitude expansion as given in [6]. Experimentally, the optical method described above might be used to extract the tilt angle of the director field. Knowing the field of the optical axis within the liquid crystal, one can calculate the distance between the real and imaginary foci shown in Fig. 5. This distance can be measured pretty well with a microscope, and from this measurement the maximum angle of the director can be extracted (Fig. 18). The comparison with the nonlinear amplitude expansion (solid line) presented in [6] at the proper frequency seems pretty good, if one takes into account that no adjustable parameters are involved in the plot.

As demonstrated above, the order parameter increases with an increase of the control parameter. This growth of the amplitude does not go beyond some limit. At a second threshold the primary patterns go unstable with respect to the formation of new ones. For these patterns the sentence stated for the primary patterns has to be repeated: The kind of instability depends on many different parameters. We like to present two examples of patterns

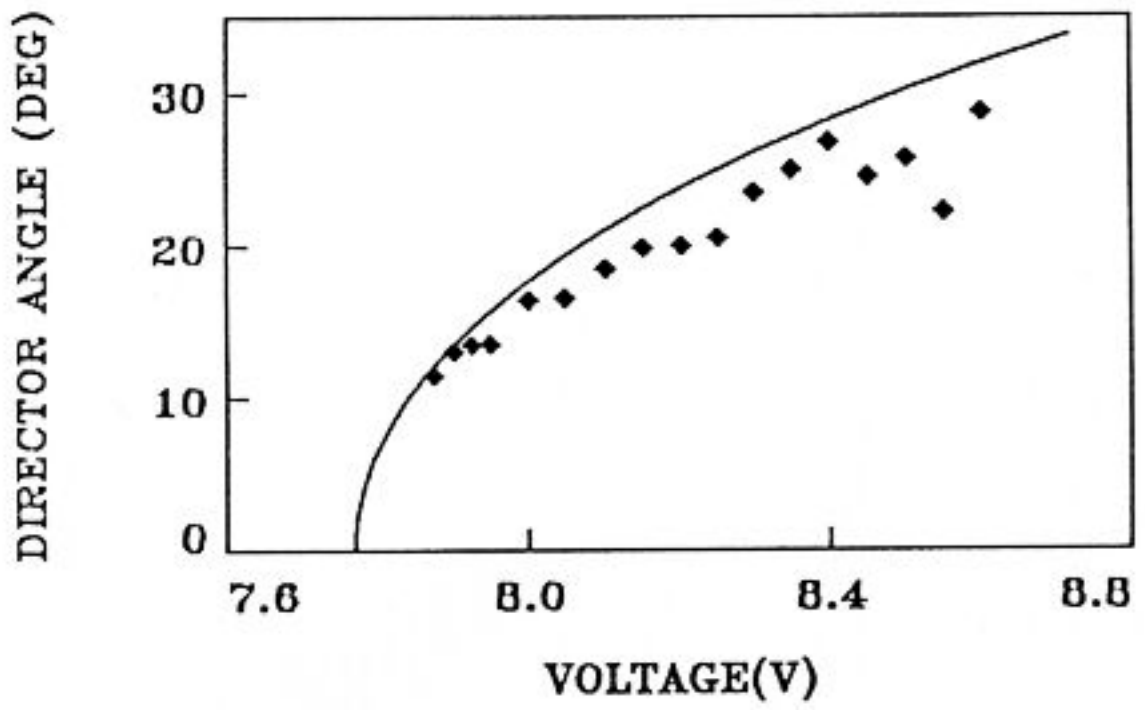

Fig. 18 Director angle obtained by measuring the distance between the real and imaginary foci. The solid line is the result of the nonlinear calculations presented in [6].

Fig. 19 The chevron pattern, the result of a secondary instability in the dielectric roll regime.

observed in the nonlinear regime: chevrons and defects. Increasing the voltage in the dielectric regime slightly above threshold leads to a characteristic flow pattern: the herringbone-like chevrons shown in the photograph 19. This pattern is unexplained theoretically, but it had been speculated [10] that its origin can be understood even by linear theory: Slightly above the first threshold linear stability analysis yields a second mode, and the superposition of these modes might be a possible explanation for the observed chevron pattern.

A characteristic feature of convection in the nonlinear regime is the existence of defects. In the following, we concentrate on the dislocations shown in Fig. 20. They are created by a secondary instability [11], which seems to have its reason in mean-flow effects. Sudden jumps in the amplitude or frequency of the driving voltage also creates this kind of imperfection of the roll

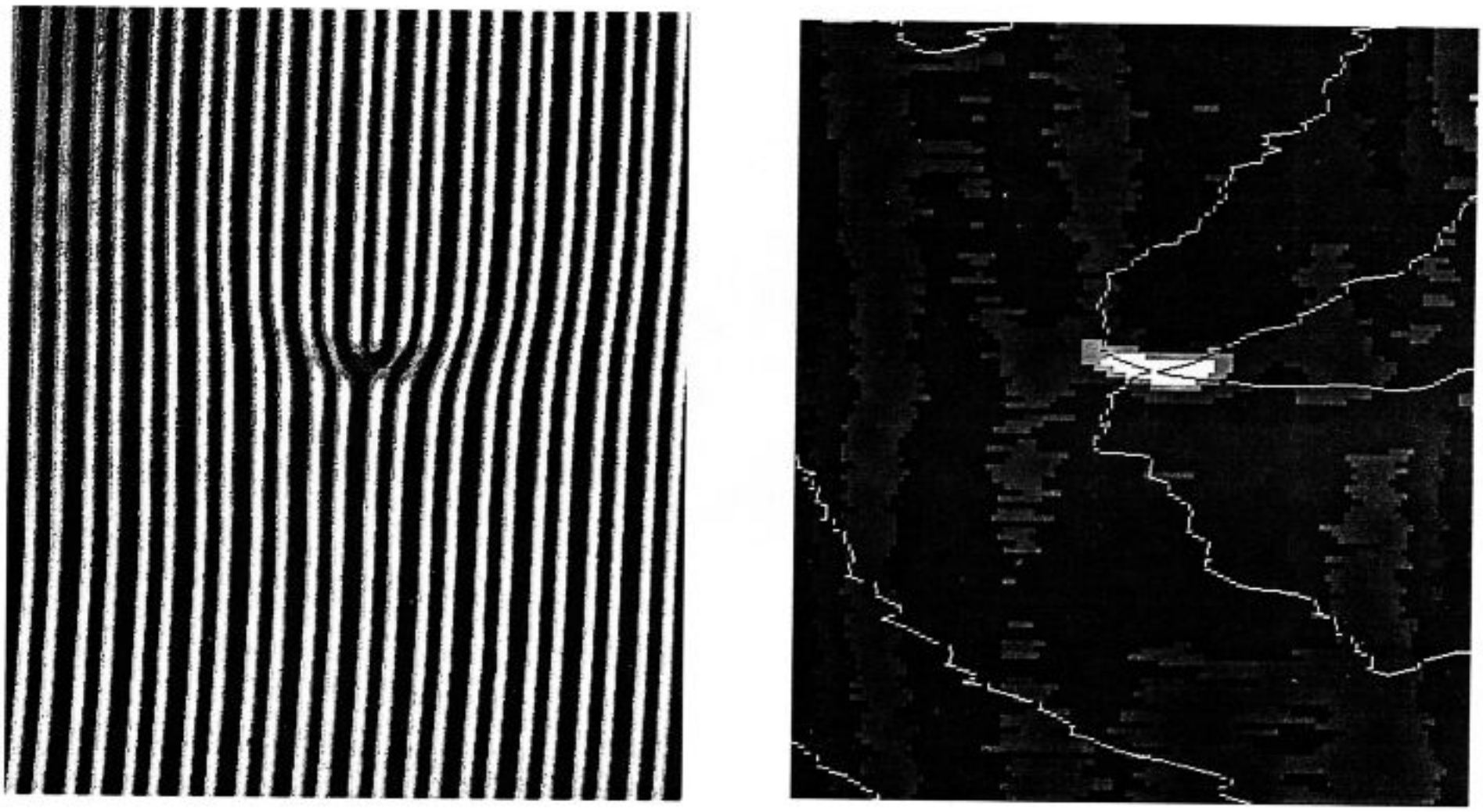

Fig. 20 The image of a defect is shown on the left hand side (virtual image). The slow modulation field extracted from this image is shown on the right hand side (black: large amplitude, white: small amplitude). The defect is located at the crossing of the zero lines of the real and the imaginary part of the slow modulation field.

pattern. In general, they are very robust and in fact hard to avoid-analogue to the process of crystal growing it is much harder to create perfect patterns than a structure accompanied by defects. Once created, the dislocations are stable at any driving voltage for topological reasons: they can annihilate in pairs only. Because they exist even slightly above threshold, they should be adequately described within the framework of a weakly nonlinear analysis, i.e. an amplitude equation. As an ansatz, one takes the linear unstable mode $\exp(ikx)$ and determines its slowly varying complex amplitude $A(x, y)$. The concept indeed leads to a realistic description of a defect. The experimentalist observes the real part of the field $A(x, y) \cdot \exp(ikx)$. The slowly varying amplitude can be extracted from this field by means of a demodulation procedure. Figure 20 shows a the magnitude of the $A(x, y)$-field, together with the lines where the real and imaginary part of this field are zero. The core of the defect is located where these lines cross.

4 Travelling Waves

Now we concentrate on one of the patterns shown in section 3, namely travelling waves (TW). As already mentioned above, they are unexplained by the theoretical calculations, but have nevertheless been observed by various experimental groups [12]. In order to discuss possible explanations for this kind of movement, let us recall a system where travelling waves are observed as well and theoretically well understood. The most popular example in the

field of fluid dynamics seems to be thermal convection in a binary mixture. Here a mixture of two fluids, say water and ethanol, is heated from below. Convection then sets in as an oscillatory instability. This is best demonstrated by pulse methods: A small (mechanical or thermal) distortion of the system leads to an oscillatory response as demonstrated in Fig. 21. A pulse of waves travelling out of the middle of the convection channel [13], where the heater is located, to the left and right of the cell is clearly seen. The reason for the oscillatory response in binary mixture convection is well understood: linear stability analysis predicts that the system goes unstable via a Hopf bifurcation, i.e. the linear growth rate contains an imaginary part.

When looking for possible explanations of the TW, one should compare to other systems as well: Taylor vortices between conical cylinders drift in a preferred direction [14], a broken left-right symmetry might induce drifting convection patterns [13], or convection patterns in a cylindrical convection cell might drift when the boundary conditions are spatially modulated [15]. We call this kind of movement drifting rolls instead of TW. They differ from the TW in the sense that they are induced by the broken symmetry of the system — they travel in one preferred direction. It is speculative but plausible to assume that non-parallel plates of the EHC-cell might lead to a drifting pattern similar to the drifting Taylor vortices between conical cylinders. In fact, it seems to be very difficult to prepare cells showing perfectly stationary rolls on the time scale presented in Fig. 12. Most often, the rolls drift with a speed of less than a wavelength/minute. One has to consider the question if the TW presented in Fig. 15 are of this drifting nature, i.e. caused by imperfections of the sample rather than by a Hopf bifurcation. One strong argument against this assumption is already the fact that the

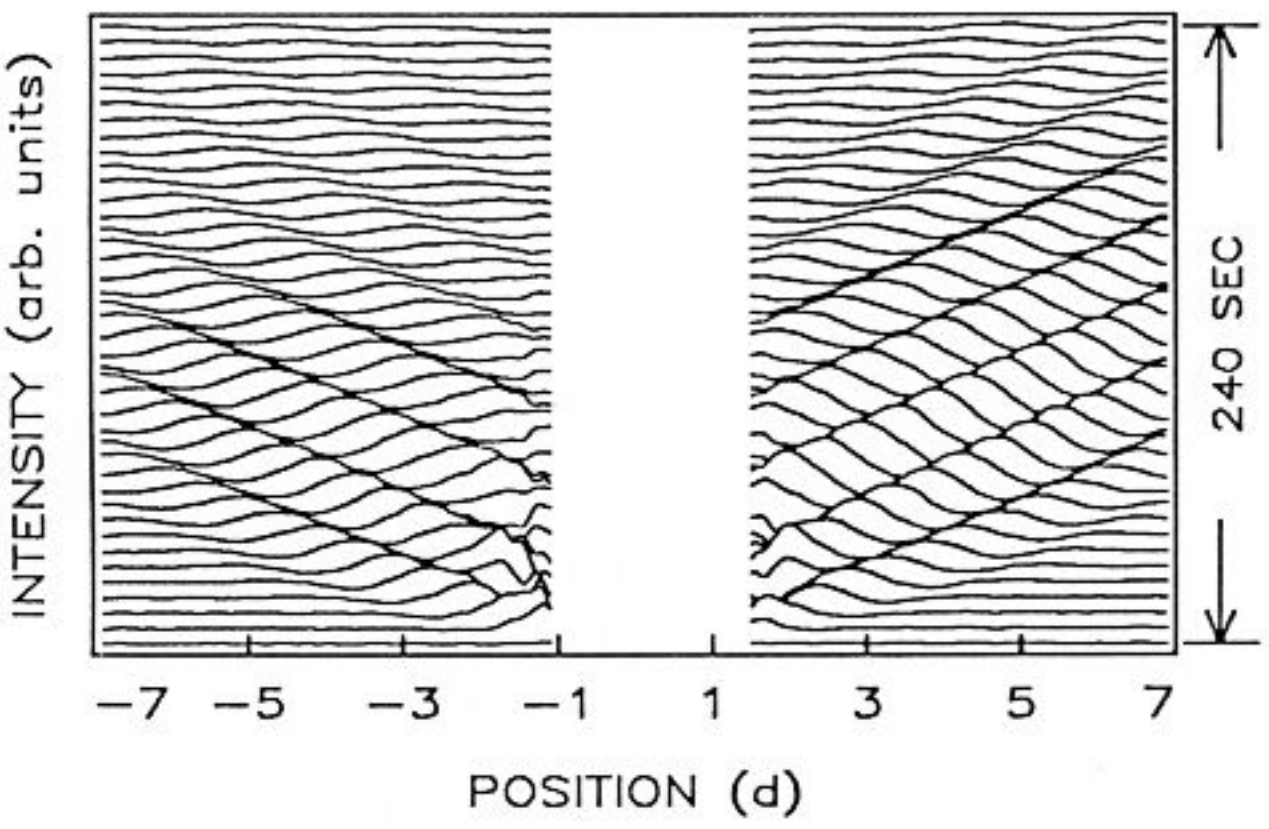

Fig. 21 Pulse of travelling waves caused by a heat pulse in a binary mixture of water and ethanol. The heater is located on the outside of the glass in the middle of the cell, where no intensity lines are visible.

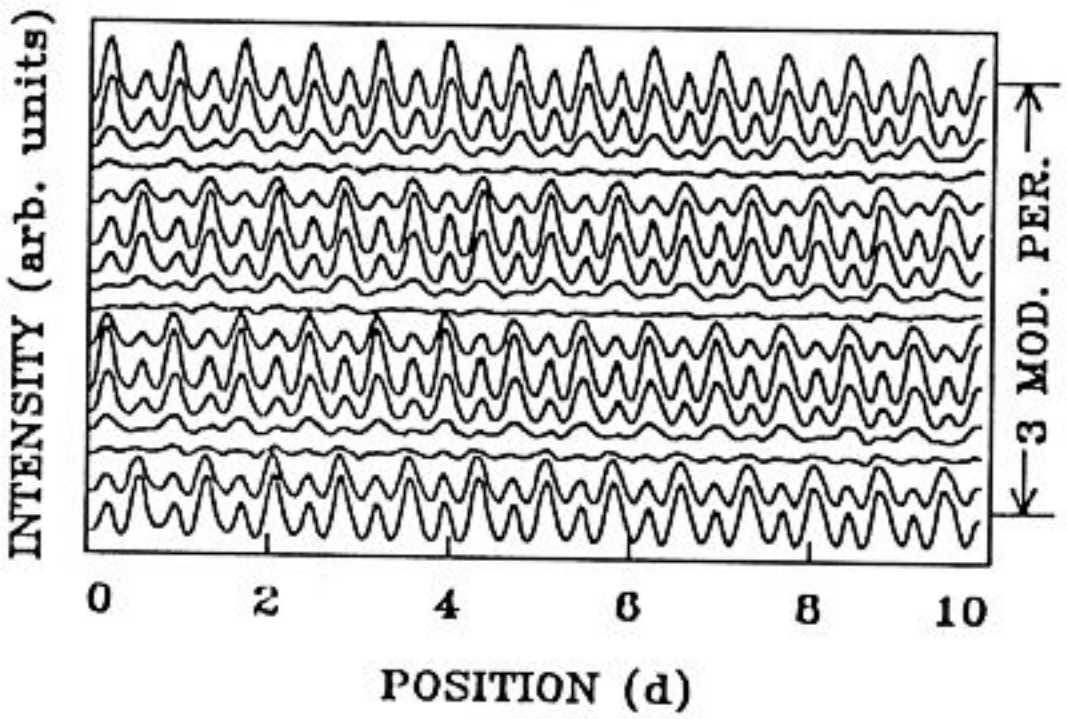

Fig. 22 Standing waves of oscillatory Williams rolls stabilized by an external modulation.

observed TW can travel in both directions and can change direction even spontaneously. Moreover, a theory concerned with the influence of a temporal modulation of the external driving on TW caused by a Hopf bifurcation supports this scenario. It was predicted, for instance, that TW should loose stability with respect to standing waves if the external frequency is close to double the linear frequency of the system [16]. This is indeed observed as demonstrated in Fig. 22. Roughly speaking, the stabilizing influence of the modulation on standing waves can be understood as follows: Both linear modes, the waves travelling to the left and the ones travelling to the right are phase locked and thus stabilized. Their superposition forms the standing wave.

Whether the external modulation leads to standing waves or not is a question of its frequency and amplitude. The phase diagram obtained with modulation is presented in Fig. 23. One has no convection on the left side of the line formed by crosses and plus signs. Convection may set in as a standing wave (diamonds) or as a travelling wave (plus). The solid line is a fit to the theoretical curve given by Riecke et al. [16]. This semiquantitative agreement between the experimental results and the ideas based on general symmetry arguments for the problem of a modulated Hopf bifurcation strongly supports the idea that a Hopf bifurcation is responsible for TW observed in EHC. Moreover, we like to point out that the modulation provides a useful tool for the measurements of the coefficents of the amplitude equation describing the TW [17].

The open circles in Fig. 23 indicate the upper bound of the standing wave state. Beyond this limit the system shows a disordered pattern consisting of nonperiodic changes in the direction of the travelling accompanied by defects [18]. This instability mechanism can be understood by a stability analysis of the coupled amplitude equations. The system is expected to go unstable with respect to the so-called Benjamin-Feir instability, which indeed has been shown to be able to produce chaotic spatio-temporal behaviour [19].

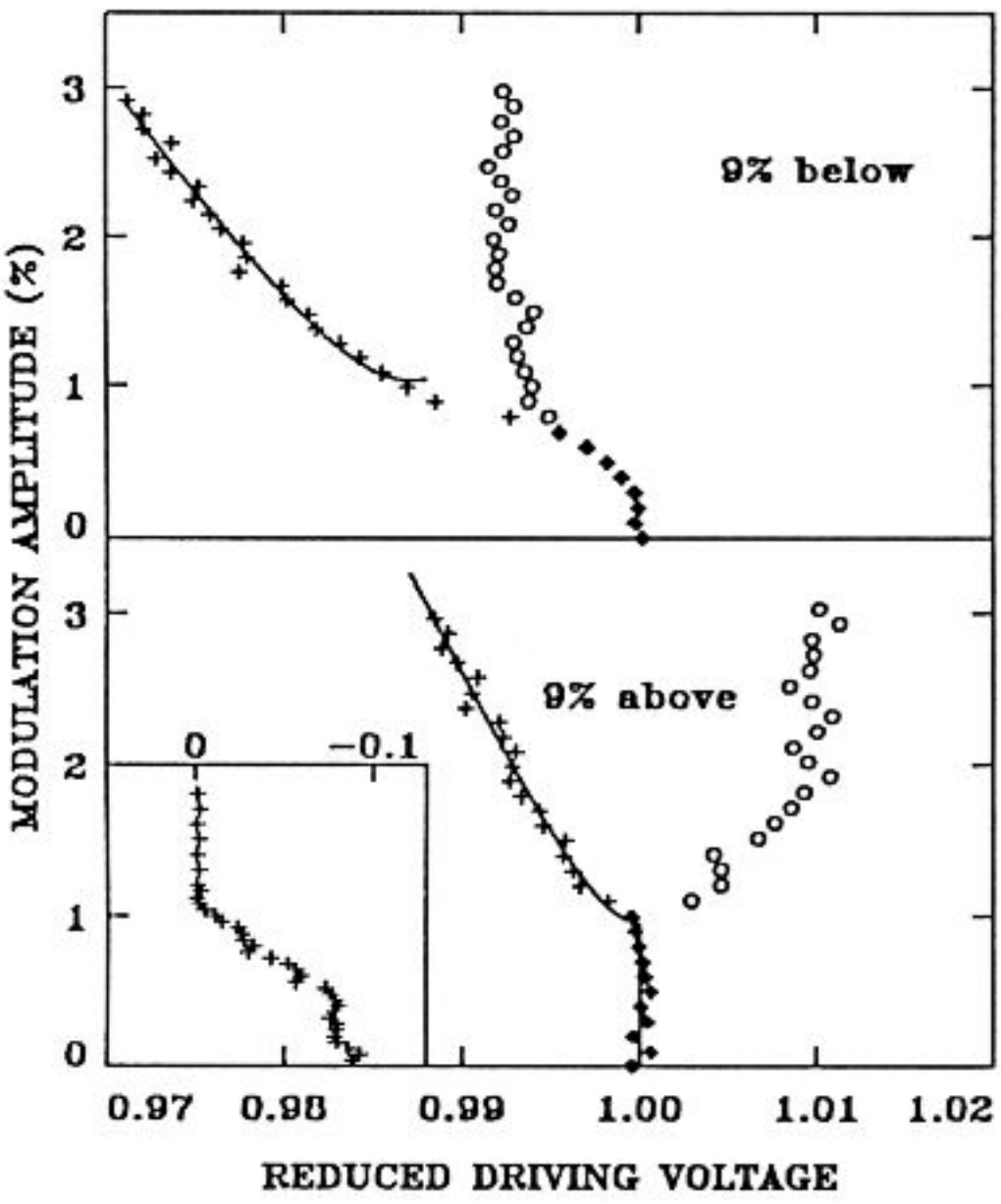

Fig. 23 Phase diagram with modulation.

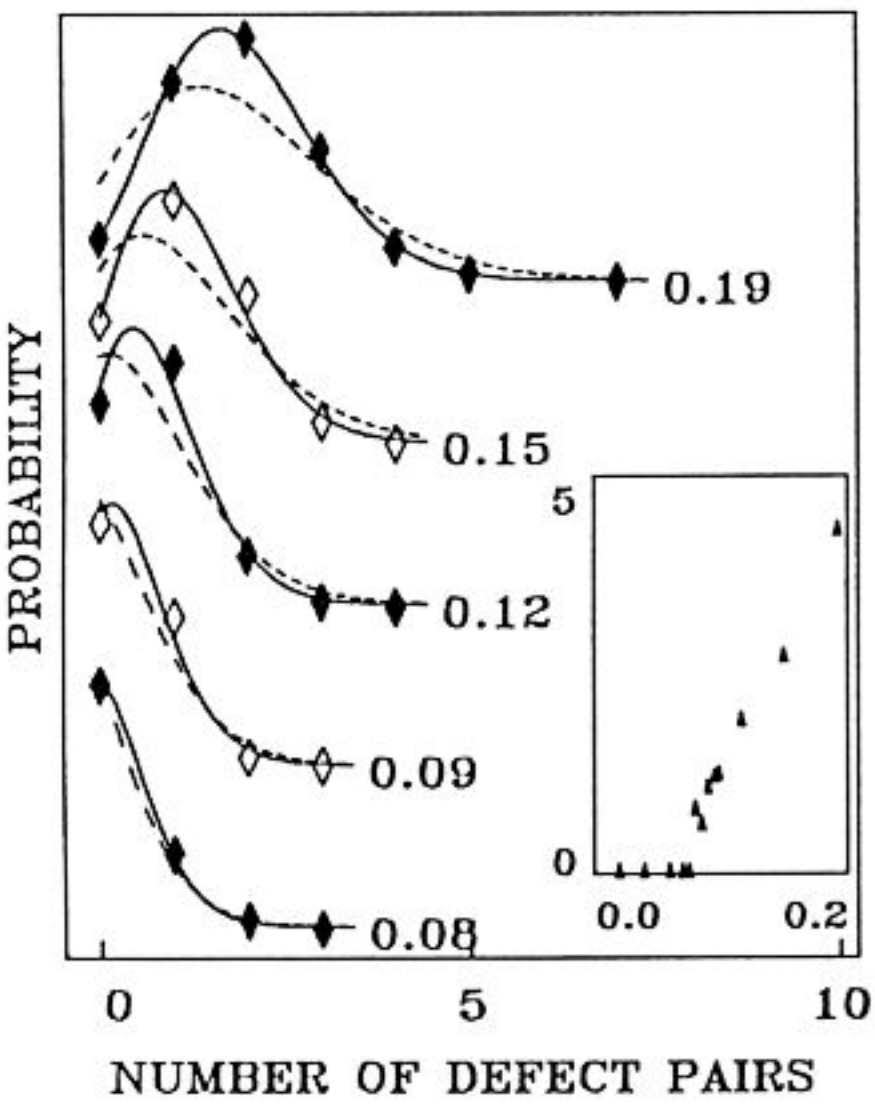

Fig. 24 Histogram of defect pairs for different driving voltages. The distribution seems well described by the solid line [20], while the dashed line (Poisson distribution) does not seem to be adequate. The inset demonstrates that the defects sets in 7.8% above threshold, thus they are very likely caused by a secondary instability.

Finally, we like to present another route to disorder. When increasing the driving voltage beyond the threshold voltage in an ordered TW state, one finds a well defined voltage where the correlation function starts to decay [12]. This is accompanied by the observation of defects. Counting these defects in a small spatial window as a function of time gives no hint for any regularity within the time series. This leads to the idea of looking for a theoretical description. Such an ansatz has been made by Gil et al. [20]. With the idea that the rate of creation of defects is a voltage-dependent constant, but the rate of annihilation processes is proportional to the number of defects squared one ends up with a distribution looking like a squared Poisson distribution for the number of defect pairs. This function is shown as a solid line in Fig. 24 together with the histograms of the numbers of pairs counted. If one takes into account that the distribution offers no adjustable parameter provided that the mean value is given the agreement can be called very good. This distribution, however, is not expected to be valid for travelling waves only. An agreement of similar quality had been found for steady convection as well [18].

5 Discussion

Obviously, electro-hydrodynamic convection in nematic liquid crystals is a very suitable candidate for experiments dealing with pattern formation and order-disorder transitions in nonequilibrium systems. This system, when compared to other fluid dynamical systems, has at least two disadvantages: There are more material parameters, and they are less well known when compared to say thermal convection in water; and the mathematical description of the instability is more complex when compared to instabilities in simple fluids.

— The most striking advantage of the system is in the shorter time scale: reaching the instability point in the double diffusive convection experiment (Fig. 21) takes about a day — the same can be achieved in EHC in less than a minute.

— The degeneracy of the wavevector present in an isotropic fluid is raised because of the preferred axis of the system. This, in principle, simplifies the theoretical description of the nonlinear state and in practice makes it simpler to perform reproducible measurements.

— The instability is driven by an *ac*-voltage whose amplitude and frequency are experimentally easily controllable parameters. By changing the amplitude a few volts the complete transition scenario from highly ordered patterns to a very disordered two-dimensional turbulent state can be studied. Changing the frequency of the applied voltage offers a degree of freedom. Thus bifurcations of higher codimension are accessible.

— The driving *ac*-field does not break the up-down symmetry of the system. This fact offers the possibility for the eigenmodes to be even or odd with respect to the middle of cell. Thus, two classes of solu-

tions (Williams rolls and dielectric rolls) become available adding to the richness of the system.
— Cells with large aspect ratios can be built allowing the observation of spatio-temporal disorder.
— Besides being well suited for studies in pattern formation the system offers the challenge to be nontrivial in nature. The interaction of hydrodynamics and electrical forces in an anisotropic fluid is a beautiful and fascinating field of physics with the additional advantage to be of technical use.
— Most important, the fascination of EHC seems to attract especially friendly people like E. Bodenschatz, L. Kramer, W. Pesch, and W. Zimmermann. We like to thank them for many helpful suggestions, patient explanations and enthusiastic support.

References

[1] *H. v. Ditfurth*, Am Anfang war der Wasserstoff. Hoffmann und Campe (Hamburg 1973)

[2] Propagation in Systems far from Equilibrium, Proceedings of the Workshop in Les Houches, France, March 1987, ed. by *J.E. Wesfreid, H.R. Brand, P. Manneville, G. Albinet, N. Boccara*; Springer Series in Synergetics, Vol. **41** (Springer, Berlin 1988) and other volumes of this series

[3] See e.g. the review of *R.C. DiPrima* and *H.L. Swinney*, in: Hydrodynamic Instabilities and the Transition to Turbulence, ed. by *H.L. Swinney* and *J.P. Gollub* (Springer, Berlin 1981)

[4] See e.g. the article of *F.H. Busse*, in: Hydrodynamic Instabilities and the Transition to Turbulence, ed. by *H.L. Swinney* and *J.P. Gollub* (Springer, Berlin 1981)

[5] See the contributions of *G. Ahlers, D.S. Cannell*, and *R.S. Heinrichs*, in: Chaos 87, International Conference on the Physics of Chaos and Systems far from Equilibrium, ed. by *M. Duong-Van* (North Holland, Amsterdam 1987) and Nuclear Physics B (Proc. Suppl.) **2** (1987); *P. Kolodner, A. Passner, H.L. Williams, C.M. Surko*, ibid.; *V. Steinberg, E. Moses, J. Fineberg*, ibid

[6] *E. Bodenschatz, W. Zimmermann*, and *L. Kramer*, J. Phys. France **49**, 1875 (1988) and references cited therein

[7] *S. Rasenat, G. Hartung, B.L. Winkler*, and *I. Rehberg*, Experiments in Fluids **7**, ? (1989)

[8] *W. Zimmermann* and *L. Kramer*, Phys. Rev. Lett. **55**, 402 (1985)

[9] *R. Ribotta, A. Joets*, and *Lin Lei*, Phys. Rev. Lett. **56**, 1595 (1986)

[10] *W. Thom*, Diploma Thesis, Bayreuth 1988; and *W. Zimmermann* and *W. Thom*, to be published

[11] *X.D. Yang, A. Joets*, and *R. Ribotta*, in: Propagation in Systems far from Equilibrium, Proceedings of the Workshop in Les Houches, France, March 1987, ed. by *J.E. Wesfreid, H.R. Brand, P. Manneville, G. Albinet, N. Boccara* (Springer, Berlin 1988)

[12] *K. Hirakawa* and *S. Kai*, Mol. Cryst. Liq. Cryst. **40**, 261 (1977); *A. Joets* and *R. Ribotta*, Phys. Rev. Lett. **60**, 2164 (1988); *I. Rehberg, S. Rasenat*, and *V. Steinberg*, Phys. Rev. Lett. **62**, 756 (1989)

[13] We used a 20% by weight concentration of ethanol in water and the experimental apparatus described in: *I. Rehberg, E. Bodenschatz, B.L. Winkler*, and *F.H. Busse*, Phys. Rev. Lett. **59**, 282 (1987)

[14] *M. Wimmer*, ZAMM **65**, T255 (1985); *M. Abboud*, ZAMM **68**, T275 (1988)

[15] *G. Hartung*, Diploma Thesis, Bayreuth 1988

[16] *H. Riecke, J.D. Crawford*, and *E. Knobloch*, Phys. Rev. Lett. **61**, 1942 (1988); *D. Walgraef*, Europhys. Lett. **7**, 485 (1988)

[17] *M. de la Torre Juarez* and *I. Rehberg*, in: New Trends in Nonlinear Dynamics and Pattern Forming Phenomena: The Geometry of Nonequilibrium, ed. by *P. Coullet* and *P. Huerre* NATO ASI Series (Plenum Press 1988)

[18] *I. Rehberg, S. Rasenat, J. Fineberg, M. de la Torre Juarez*, and *V. Steinberg*, Phys. Rev. Lett. **61**, 2449 (1988)

[19] *A.C. Newell*, in: Propagation in Systems far from Equilibrium, Proceedings of the Workshop in Les Houches, France, March 1987, ed. by *J.E. Wesfreid, H.R. Brand, P. Manneville, G. Albinet, N. Boccara* (Springer, Berlin 1988), and references cited therein. The fact that modulated TW go unstable via this mechanism has been demonstrated by *W. Zimmermann*, to be published

[20] *L. Gil, J. Lega*, and *J.L. Meunier* (to be published)